Terrestrial records of glacial terminations V and IV and insights on deglacial mechanisms

F. Marra[1]*, A. Pereira[2,3], B. Jicha[4], S. Nomade[5], I. Biddittu[6], F. Florindo[1], G. Muttoni[7], E.M. Niespolo[8,9], P.R. Renne[8,9], V. Scao[5]

[1] Istituto Nazionale di Geofisica e Vulcanologia, Rome, Italy
[2] Université Paris-Saclay, CNRS UMR 8148, GEOPS, France
[3] Département Hommes et environnements, Muséum national d'Histoire naturelle, Paris, France
[4]Department of Geoscience, University of Wisconsin-Madison, USA
[5] CEA Saclay, LSCE, UMR-8212, UVSQ-IPSL et Université Paris Saclay, Gif-sur-Yvette Cedex, France
[6] Istituto Italiano di Paleontologia Umana, Anagni, Italy
[7] Department of Earth Sciences, University of Milan, Milan, Italy
[8] Department of Earth and Planetary Science, University of California, Berkeley, USA
[9] Berkeley Geochronology Center, Berkeley, USA

*Corresponding author: fabrizio.marra@ingv.it
ORCID ID 0000-0002-4881-9563

Supplementary Material #1A - ^{40}Ar-^{39}Ar full methods

Samples for ^{40}Ar/^{39}Ar analyses, both those dated for the present study and those from previous literature, were prepared at the Laboratoire des Sciences du Climat et de l'Environnement facility (CNRS-CEA, Gif-sur-Yvette), France, and at the University of Wisconsin-Madison.

Three distinct irradiations have been performed and the samples were dated in three facilities (Berkeley Geochronology Center, USA), Laboratoire des Sciences du Climat et de l'Environnement (CEA, Saclay), WiscAr Laboratory of Wisconsin University (USA).

For the previously dated samples we remand to Marra et al. (2020) (CA-GCT, CA-C1), Pereira et al. (2018) (Isoletta 1, Isoletta 2, Isoletta 3, Lademagne 1, Lademagne 2, Cava Pompi), and Nomade et al. (2011) (Ceprano).

All the ages reported in the main text have been (re)calibrated to ACs standard age of 1.1848 Ma (Niespolo et al., 2017).

Sample preparation protocol

Whole rock samples prepared at the Laboratoire des Sciences du Climat et de l'Environnement facility (CEA Saclay, France) were crushed, sieved and then cleaned in distilled water in an ultrasonic bath. Clean portions coarser than 840 μm (> 20mesh) and ranging between 840 and 600 μm (30-20 mesh) were selected to extract suitable minerals. When available, at least 50 transparent and unaltered K-feldspars were carefully handpicked under a binocular for each sample after a magnetic separation. When it was possible to recognize unaltered ones, leucites were also picked. To eliminate potential adhering groundmass residues on the selected minerals, the latter were finally leached with a 5-7 % HF acid solution and cleaned several times using distilled water in an ultrasonic bath.

Samples prepared at the University of Madison were crushed and sieved to a 250-500 μm size fraction. Inclusion-free sanidine was isolated using a Frantz magnetic separator and hand-picking under a binocular microscope. The selected crystals were cleaned for 3 min in a 10% HF solution and then rinsed repeatedly in deionized water.

Irradiations

Samples PO-C6, BL-1A, BL-5, and PI-1, PI-2 were irradiated for one hour and two hours respectively in the Cd-lined, in-core CLICIT facility of the Oregon State University TRIGA reactor (IRR number 482 and IRR COO2). Standard flux monitor ACs-2 were co-irradiated to calculate the neutron fluence (J value) for each sample. Interference corrections were based on the following nucleogenic production ratios (Renne et al., 2015): $(^{40}Ar/^{39}Ar)_K = (7.30 \pm 0.92)10^{-4}$; $(^{37}Ar/^{39}Ar)_K = (2.24 \pm 0.16)10^{-4}$; $(^{38}Ar/^{39}Ar)_K = (1.196 \pm 0.013)10^{-2}$; $(^{39}Ar/^{37}Ar)_{Ca} = (7.02 \pm 0.12)10^{-4}$; $(^{36}Ar/^{37}Ar)_{Ca} = (2.702 \pm 0.004)10^{-2}$; $^{36}Cl/^{38}Cl = (2.628 \pm 0.002)10^{2}$.

Samples BL-4, CE-1, and CE-2 were irradiated for 1.5 hours in the Cd-lined, in-core CLICIT facility of the Oregon State University TRIGA reactor. Neutron flux monitor ACs-2 was co-irradiated with the sample. Interference corrections were based on the following nucleogenic production ratios (Jicha and Brown, 2014; Renne et al., 2013): $(^{40}Ar/^{39}Ar)_K = (5.40 \pm 1.40)10^{-4}$; $(^{37}Ar/^{39}Ar)_K = (2.24 \pm 0.16)10^{-4}$; $(^{38}Ar/^{39}Ar)_K = (1.210 \pm 0.022)10^{-2}$;

$(^{39}Ar/^{37}Ar)_{Ca}$ =(6.95 ± 0.09)10^{-4}; $(^{36}Ar/^{37}Ar)_{Ca}$ =(2.65 ± 0.002)10^{-2}; $^{36}Cl/^{38}Cl$ = (2.628 ± 0.002)10^{2}.

BGC analytical processes

Analyses for samples PO-C6, BL-1A, BL-5 were conducted at the Berkeley Geochronology Center (BGC, USA) using a MAP 215 mass spectrometer (MAP 1) equipped with a Nier-type source, a Balzers electron multiplier detectors and retractable Faraday cups. After irradiation, samples were separately transferred into a UHV chamber mounted in an automated x-y stage. Crystals were then totally fused using a CO_2 laser (7 Watts) in order to extract the argon. The extracted gas was then purified of other gases on a fully-automated line equipped with two C-50 getters and a cryogenic condensation trap. Ion beams were measured both using magnetic field switching to cyclically measure all argon isotopes from ^{36}Ar to ^{40}Ar in 15 cycles of peak-hopping on the electron multipliers operated in analog mode. For each sample neutron J fluence was calculating using co-irradiated flux standards Alder Creek Sanidine (ACs-2, Nomade et al., 2005) with an age of 1.1848 ± 0.0006 Ma (1σ, Niespolo et al., 2017) and the K total decay constant of Min et al., (2000). J values calculated for each sample are the following: BL-1A: J=2.548 E -04 ± 4.06 E -07, P0-C6: J= 2.577 E -04 ± 3.67 E -07, BL-5: J= 2.549 E -04 ± 5.29 E -07. Procedural blank measurements were performed before and after every unknown. Individual blanks were 4-5 × 10^{-16}, 8-9 × 10^{-18}, and 1-2 × 10^{-19} mol for ^{40}Ar, ^{39}Ar and ^{36}Ar, respectively. Because the variation in the time series of blanks exceeds the uncertainty in a single blank measurement, blank corrections to data require fitting to account for variability in blanks. We use a simple arithmetic mean and standard deviation of ~40 to 100's blank measurements over time throughout the analytical sequence to blank-correct bracketed unknown sample measurements (Supp. File 1). Mass discrimination was calculated based on automated analyses of air pipettes between every five single-grain analyses (plus intercalated blanks) using air pipette data based on a power law correction (Renne et al., 2009) and the atmospheric $^{40}Ar/^{36}Ar$ value of 298.56 (Lee et al, 2006). Measurements and data reduction were made using the

software mass-spec developed by BGC and run on a Macintosh computer (Mass Spec, version 8.132; A. Deino).

LSCE analytical processes

After irradiations, samples PI-1 and PI-2 analyzed at the Laboratoire des Sciences du Climat et de l'Environnement (CEA, Saclay) were separately transferred in a copper sample holder and put into a double vacuum window. Crystals were individually fused using a CO2 laser (25 W, using 10% of the nominal power). Extracted gases were purified by two GP 110 getters (ZrAl) and argon isotopes measured using a micromass 5400 mass spectrometer equipped with an electron multiplier Balzers 217 SEV SEN coupled with an ion counter (full analytical protocol is detailed in Nomade et al., 2010). Neutron J fluence for each sample was calculating using co-irradiated Alder Creek Sanidine (ACs-2, Nomade et al., 2005) with an age of 1.1891 ± 0.0008 Ma (1σ, Niespolo et al., 2017) and the K total decay constant of Renne et al., (2011). Procedural blank measurements were performed after every three unknown samples. Mass discrimination correction was monitored by measurements of air argon of various beam sizes and was calculated relative to a 40Ar/36Ar ratio of 298.56 (Lee et al., 2006). Ages provided were finally recalculated according an age of 1.1848 ACs ± 0.0006 Ma (1σ, Niespolo et al., 2017) to be consistent with the main text.

University of Wisconsin-Madison analytical processes

Analyses for samples CE-1, CE-2 and BL-4 were conducted at the WiscAr Laboratory using a Noblesse 5-collector mass spectrometer. Individual crystals were fused using a 50W CO_2 laser, and the extracted gas was then cleaned using two GP-50 getters and a cryogenic condensation trap. Analytical routine follows that described in Jicha et al. (2016). For each sample neutron fluence parameter J was calculating using co-irradiated flux standards Alder Creek Sanidine (ACs = 1.1864 Ma; Jicha et al., 2016) and the K total decay constant of Min et al., (2000). Procedural blank measurements were performed after every unknown. The atmospheric values of Lee et al, (2006) were used for age calculations.

REFERENCES

Jicha, B.R., B.S. Singer, and P. Sobol (2016), Re-evaluation of the ages of 40Ar/39Ar sanidine standards and supereruptions in the western U.S. using a Noblesse multi-collector mass spectrometer, Chemical Geology 431, 54–66.

Jicha, B.R., Brown, F.H., 2014. An age for the Korath Range, Ethiopia and the viability of 40Ar/39Ar dating of kaersutite in Late Pleistocene volcanics Quaternary Geochronology 21, 53-57. DOI: 10.1016/j.quageo.2013.03.007

Kuiper, K.F., Deino, A., Hilgen, F.J., Krijgsman, W., Renne, P.R., Wijbrans, J.R., 2008. Synchronizing Rock Clocks of Earth History, Science 320, 500 – 504.

Lee, J.Y., Marti, K., Severinghaus, J.P., Kawamura, K., Hee--Soo, Y., Lee, J.B., Kim, J.S., 2006. A redetermination of the isotopic abundances of atmospheric Ar. Geochimica et Cosmochimica Acta 70, 4507-4512. doi:10.1016/j.gca.2006.06.1563.

Min, K.W., Mundil, R., Renne, P.R., Ludwig, K.R., 2000. A test for systematic errors in 40Ar/39Ar geochronology through comparison with U/Pb analysis of a 1.1-Ga rhyolite. Geochim. Cosmochim. Acta 64, 73-98.

Niespolo, E.M., Rutte, D., Deino, A.L., & Renne, P.R., 2017, Intercalibration and age of the Alder Creek sanidine $^{40}Ar/^{39}Ar$ standard, Quaternary Geochronology 39, 205 – 213, doi: 10.1016/j.quageo.2016.09.004

Nomade, S., Renne, P.R., Vogel, N., Deino, A.L., Sharp, W.D., Becker, T.A., Jaouni, A.R., Mundil, R., 2005. Alder Creek sanidine (ACs-2): a Quaternary 40Ar/39Ar dating standard tied to the Cobb Mountain geomagnetic event. Chem. Geol. 218, 315-338.

Nomade, S., Gauthier, A., Guillou, H., Pastre, J.F., 2010. 40Ar/39Ar temporal framework for the Alleret maar lacustrine sequence (French Massif Central): volcanological and Paleoclimatic implications. Quat. Geochronol. 5, 20-27.

Renne P. R., Deino A. L., Hames, W.E., Heizler, M.T., Hemming, S.R., Hodges, K.V., Koppers, A.a.P., Mark, D.F., Morgan, L.E., Phillips, D., Singer, B.S., Turrin, B.D., Villa, I.M., Villeneuve, M., Wijbrans, J.R., 2009. Data reporting norms for $^{40}Ar/^{39}Ar$ geochronology. Quaternary Geochronology 4, 346–352.

Renne, P.R., Deino, A.L., Hilgen, F.J., Kuiper, K.F., Mark, D.F., Mitchell III, W.S., Morgan, L.E., Mundil, R., Smit, J. 2013. Time scales of critical events around the cretaceous-Paleogene boundary. Science 339 (6120), 684-687.

Renne, P.R., Sprain, C.J., Richards, M.A., Self, S., Vanderkluysen, L., Pande, K., 2015. State shift in Deccan volcanism at the Cretaceous-Paleogene boundary, possibly induced by impact. Science 350, 76-78.

Terrestrial records of glacial terminations V and IV and insights on deglacial mechanisms

F. Marra[1]*, A. Pereira[2,3], B. Jicha[4], S. Nomade[5], I. Biddittu[6], F. Florindo[1], G. Muttoni[7], E.M. Niespolo[8,9], P.R. Renne[8,9], V. Scao[5]

[1] Istituto Nazionale di Geofisica e Vulcanologia, Rome, Italy
[2] Université Paris-Saclay, CNRS UMR 8148, GEOPS, France
[3] Département Hommes et environnements, Muséum national d'Histoire naturelle, Paris, France
[4]Department of Geoscience, University of Wisconsin-Madison, USA
[5] CEA Saclay, LSCE, UMR-8212, UVSQ-IPSL et Université Paris Saclay, Gif-sur-Yvette Cedex, France
[6] Istituto Italiano di Paleontologia Umana, Anagni, Italy
[7] Department of Earth Sciences, University of Milan, Milan, Italy
[8] Department of Earth and Planetary Science, University of California, Berkeley, USA
[9] Berkeley Geochronology Center, Berkeley, USA

*Corresponding author: fabrizio.marra@ingv.it
ORCID ID 0000-0002-4881-9563

Supplementary Mayerial #1B - Age data and interpretations

1. Dating of detrital minerals in sedimentary deposits

40Ar/39Ar single-grain dating of detrital minerals has been used in regional-scale provenance studies on the erosional record, as well as in reconstructing the exhumation processes (e.g., Brewer et al., 2003; Ruhl and Hodges, 2005; Germignani et al., 2018, 2019; Malusà and Garzanti, 2019). More recently, Marra et al. (2019) have used cooling ages of detrital sanidine grains extracted from sedimentary deposits in central Italy to provide *terminus post-quem* (maximum ages) to the time of their deposition, aimed at establishing correlation of Tyrrhenian Sea coastal terraces with Marine Isotope Stage (MIS) sea-level highstands. Application of such method relies on the exceptional deliverance of k-rich eruptive products during the Middle-Upper Pleistocene activity of the volcanic districts of the Roman Magmatic Region (central Italy), which includes the volcanic districts of Vulsini, Vico, Monti Sabatini, Colli Albani, Volsci, Roccamonfina, Phlegraean Fields and Somma-Vesuvio (Peccerillo, 2017). In particular, sanidine represents a mineral species characterized by high resistance to mechanical and chemical alteration, which is largely present in these volcanic products (Peccerillo, 2017, and references therein). Due to the continuous eruptive activity that characterized this volcanic region during this time span, dating of sedimentary samples has revealed an extremely useful tool to assess the age of aggradational successions deposited in response to sea-level rise during glacial terminations (Marra et al., 2016 and ref. therein) in the absence of intercalated, primary tephra layers (see Marra et al., 2019, for an in-depth discussion). In fact, when a statistically significant number of crystals is

dated (i.e., 30-40 grains), it is reasonable to assume that the age of the youngest crystal population, besides providing a maximum age for the sedimentary deposit, also should be regarded as documenting the lack of crystals from younger eruptive products, providing a minimum age (*terminus ante-quem*) to the time of deposition. As discussed in Marra et al. (2019), the youngest eruptions should be better represented in reworked, sedimentary deposits because their products crop out in wider areas than the old ones, which are buried under a longer sequence of strata. This consideration supports the principle that the age of a layer is bracketed between the ages of its youngest crystal population and of the next younger eruption, whose crystals do not occur in the layer but is widely documented in the area.

Hereby we discuss the interpretation of the maximum ages derived from dating of four sedimentary samples: CA-CGT (dated in Marra et al., 2021), CE-1, CE-2, BL-5 (dated in the present study).

1.1 Sample CA-CGT

24 crystals extracted from the sand matrix of a ca. 2 m thick gravel layer cropping out at Colle Avorone locality (Sample CA-CGT) were dated by Marra et al. (2021). 3 youngest crystals provided a weighted mean age of 359.5±6.5 ka (2σ uncertainty). Other 21 crystals provided two groups of ages, the largest one (14 grains) ranging 359 - 450 ka, with other six crystals spanning 700 - 850 ka. The younger group of ages matches the duration of the main eruptive phase occurred at the Volsci Volcanic Field (VVF) 424±13– 349.5±5.0 ka (Marra et al., 2021).

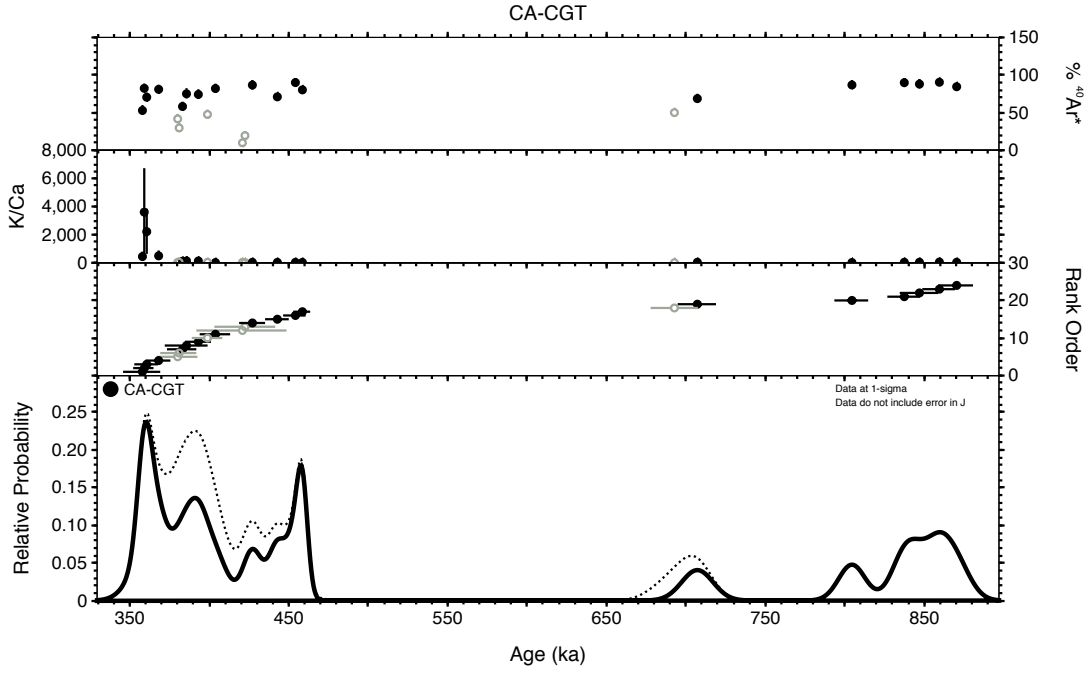

Figure S1. Open circles indicate crystals with 40Ar* <50% which are excluded from the statistics (full black line in inset d) (see Marra et al., 2021 for discussion).

Regarding the older crystal ages, it should be noted that five samples from phreatomagmatic deposits analyzed in Marra et al. (2021) yielding weighted

mean ages in the interval 761.5±9.5 - 349.5±5.0 ka evidenced significant dispersion towards old ages (Figure S2). These products were mainly sourced from isolated, monogenetic eruptive centers. Therefore, it is unlikely that the older age values might have derived from earlier buried volcanic edifices or erupted deposits, and yet may provide evidence of older magma batches that cooled in sub-surface conditions.

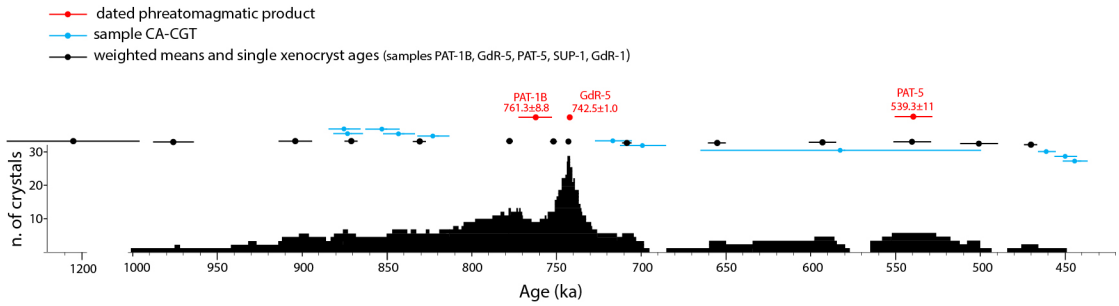

Figure S2 - Histogram showing crystal age distribution of the dated samples.

Samples CE-1, CE-2 (this work)

Sample CE-1 was collected in borecore Ceprano 1 at 39.3 m depth within a coarse gravel layer with abundant sand matrix. The youngest crystal out of a population of 30 extracted from this sediment yielded a 40Ar/39Ar age of 452.4±1.8 ka (2σ uncertainty). Sample CE-2 was collected at 15.1 m depth in borehole Ceprano 2, at the base of a coarse sand layer and yielded a youngest crystal date of 389.6±2.7 ka (2σ uncertainty).

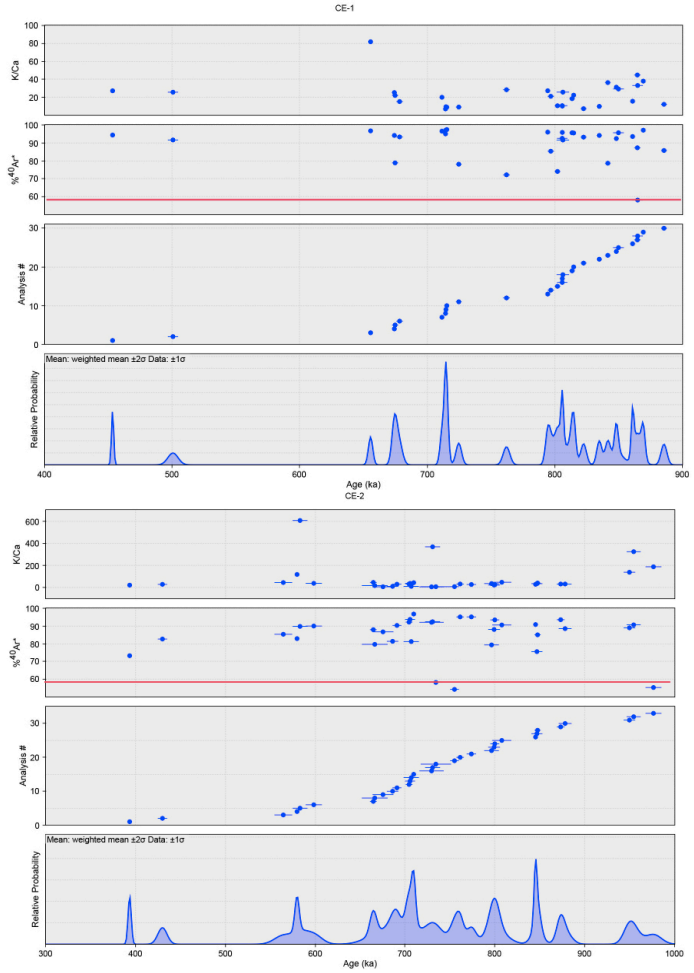

Figure S3 – Relative probability diagrams of crystal ages for samples CE-1, CE-2.

These two maximum ages can be regarded as statistically significant even if based on one single crystal. The Ceprano boreholes were drilled in Campogrande which is located on the left hydrographic side of the Sacco catchment basin, a sector draining the most active and densely vent-populated volcanic area of the Volsci Volcanic Field. A climactic eruptive phase occurred at the VVF in the interval 420 - 350 ka[9], so the lack of crystals younger than 453 ka is strongly suggesting that the emplacement of the sand deposit occurred before the start of this volcanic phase. Consistent with this hypothesis, there is one crystal of 428±10 ka along one youngest crystal of 390±3.6 ka in the sample stratigraphically above. Moreover, these two ages along with that of 350.8±8 ka on the primary layer occurring at the top of the sedimentary succession recovered in the Ceprano boreholes (Nomade et al., 2011) provide a constant sedimentation rate of 38 cm/ky (see Figure 4 in the main text), which accounts for the exactness of these ages.

Therefore, it is reasonable to assume that also the maximum ages derived from reworked sanidine crystals can be regarded as providing precise time constraints to sediment deposition, as the one on the primary volcanic layer. Indeed, and age close to 453 ka for the gravel deposition during MIS 11 is in perfect agreement with the constraints provided from the Paleo-Tiber aggradational successions, which bracket it between 451±2 and 445±3 ka (Marra et al., 2021, see Figure 8 in the main text).

Sample BL-5 (this work)

Sample BL-5 was collected in a sandy-clayey travertine layer embedding several sub-cm sized, very altered volcanic scoriae. Crystal extracted from this sample yielded two distinct groups of ages.

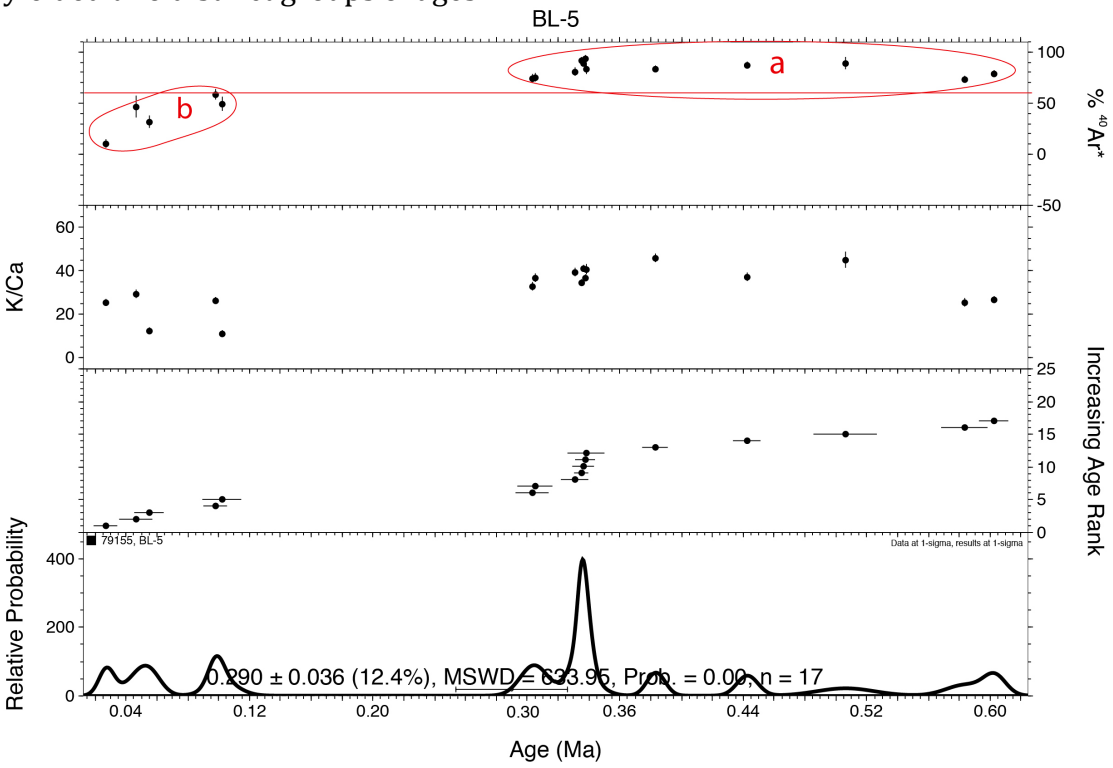

Figure S4 - Relative probability diagram of crystal ages for sample BL-5

One group of older ages ranging 300 - 600 ka ("a") is consistent with expected distribution for a deposit reworking the volcanic deposit of the Volsci Volcanic Field (VVF), the activity of which broadly spanned the interval 750-250 ka, as also observed in the sedimentary samples CE-1 and CE-2 (see Figure S2). The occurrence of one second group of ages ranging 120 - 30 ka ("b") is problematic to explain, given the much unlikely circumstance that it may reflect the real age of the deposit. Indeed, the travertine layer occurs on top of the "lower lacustrine succession", closely constrained at this location by tephra ages of 538 and 517 ka, and is part of the "upper fluvial-lacustrine succession" which previous (Devoto, 1965) and the present study constrain between 390 and ca. 300 ka. Therefore, two hypotheses can be made to explain the second group of crystal ages.

The anomalously young ages most probably represent much younger ash fall and/or eolian material that was worked into the deposit through fractures; indeed, the sampled deposit was exposed on a slightly inclined surface in the middle of a hillside, which is affected by continuous sliding of reworked sediments from the uphill section.

Alternatively, these anomalous young ages may result from contamination in the field or laboratory.

In any case, we consider the weighted mean age of 300±12 ka yielded by the two youngest crystals in group "a" as a reliable maximum age for the deposit.

REFERENCES

Brewer, I.D., Burbank, D.W., Hodges, K.V., 2003. Modelling detrital cooling-age populations: Insights from two Himalayan catchments. Basin Res. 15 (3), 305–320. https://doi.org/10.1046/j.1365-2117.2003.00211.x.

Devoto, G.,1965. Lacustrine Pleistocene in the lower Liri Valley (southern Latium). Geologica Romana 4, 291–368.

L. Gemignani, K.F. Kuiper, J.R. Wijbrans, Xilin Sun, A. Santato, 2019. Improving the precision of single grain mica 40Ar/39Ar-dating on smaller and younger muscovite grains: Application to provenance studies. Chemical Geology 511 (2019) 100–111.

Gemignani, L., van der Beek, P.A., Braun J., Najman, Y., Bernet, M., Garzanti, E. Wijbrans, J.R., (2018). Downstream evolution of the thermochronologic age signal in the Brahmaputra catchment (eastern Himalaya): Implications for the detrital record of erosion. Earth Planet. Sci. Lett.s499, 48–61, doi:https://doi.org/10.1016/j.epsl.2018.07.019.

Malusà, M.G., Garzanti, E., 2019. the sedimentology of detrital thermochronology. In: Malusà, M.G., and Fritzgerald (eds.), Fission-Tracks Thermochronology and its Application to Geology, Springer textbook in Earth Sciences. Geography and Environment. https://doi.org/10.1007/978-3-319-89421-8_7.

Marra, F., Rohling, E.J., Florindo, F., Jicha, B., Nomade, S., Pereira, A., Renne, P.R., 2016a. Independent 40Ar/39Ar and 14C age constraints on the last five glacial terminations from the aggradational successions of the Tiber River, Rome (Italy). Earth Planet Sci. Lett. 449, 105-117. doi:10.1016/j.epsl.2016.05.037

Marra, F. Gaeta, M. Jicha, B.R. Nicosia, C. Tolomei, C. Ceruleo, P. Florindo, F. Gatta, M. La Rosa, M. Rolfo, M.F., 2019b. MIS 9 to MIS 5 terraces along the Tyrrhenian Sea coast of Latium (central Italy): assessing interplay between sea-level oscillations and tectonic movements, Geomorphology 346: 106843. DOI:10.1016/j.geomorph.2019.106843

Marra, F., Cardello, L., Gaeta, M., Jicha, B., Montone, P., Niespolo, E., Nomade, S., Palladino, D.M., Pereira, A., De Luca, G., Florindo, F., Frepoli, A., Renne, P., Sottili, G., 2021. The Volsci Volcanic Field (central Italy): an open window on continental subduction processes, International Journal of Earth Sciences 110:689–718. DOI:10.1007/s00531-021-01981-6

Nomade, S., Muttoni, G., Guillou, H., Robin, E. & Scardia, G., 2011. First $^{40}Ar/^{39}Ar$ age of the Ceprano man (central Italy). *Quat. Geochronol.* 6, 453-457.

Marra, F., Pereira, A., Boschian, G., Nomade, S., 2021. MIS 13 and MIS 11 aggradational successions of the Paleo-Tiber delta: geochronological constraints to sea-level fluctuations and to the Acheulean sites of Castel di Guido and Malagrotta (Rome, Italy), Quaternary International

Peccerillo, A. Cenozoic Volcanism in the Tyrrhenian Sea Region in Advances in Volcanology, pp. 399; 10.1007/978-3-319-42491-0 (Springer International Publishing, 2017).

Ruhl, K.W., Hodges, K.V., 2005. The use of detrital mineral cooling ages to evaluate steady state assumptions in active orogens: an example from the central Nepalese Himalaya. Tectonics 24 (4), 1–14. https://doi.org/10.1029/2004TC001712.

Terrestrial records of glacial terminations V and IV and insights on deglacial mechanisms

F. Marra[1]*, A. Pereira[2,3], B. Jicha[4], S. Nomade[5], I. Biddittu[6], F. Florindo[1], G. Muttoni[7], E.M. Niespolo[8,9], P.R. Renne[8,9], V. Scao[5]

[1] Istituto Nazionale di Geofisica e Vulcanologia, Rome, Italy
[2] Université Paris-Saclay, CNRS UMR 8148, GEOPS, France
[3] Département Hommes et environnements, Muséum national d'Histoire naturelle, Paris, France
[4]Department of Geoscience, University of Wisconsin-Madison, USA
[5] CEA Saclay, LSCE, UMR-8212, UVSQ-IPSL et Université Paris Saclay, Gif-sur-Yvette Cedex, France
[6] Istituto Italiano di Paleontologia Umana, Anagni, Italy
[7] Department of Earth Sciences, University of Milan, Milan, Italy
[8] Department of Earth and Planetary Science, University of California, Berkeley, USA
[9] Berkeley Geochronology Center, Berkeley, USA

*Corresponding author: fabrizio.marra@ingv.it
ORCID ID 0000-0002-4881-9563

Supplementary Material #3 - Stratigraphic sections

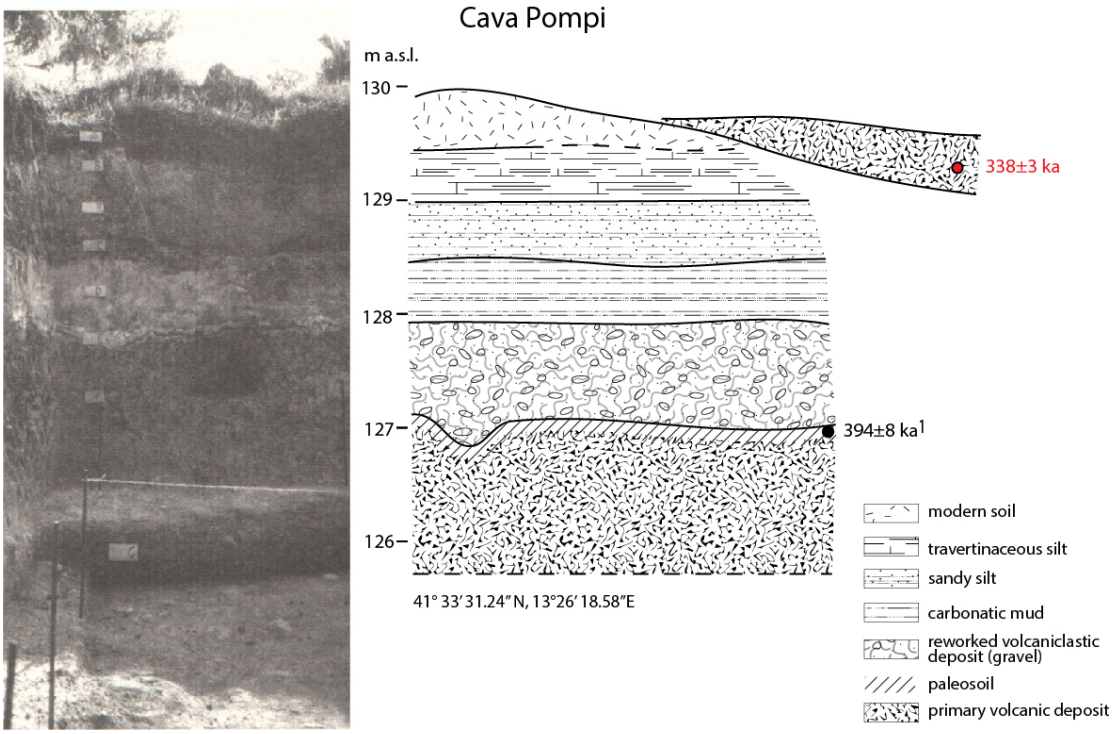

Figure S5 - Stratigraphic sketch of Cava Pompi archaeological section. Original photograph taken by author I. Biddittu. In red, $^{40}Ar/^{39}Ar$ age performed for the present study. References: (1) Pereira et al., 2018.

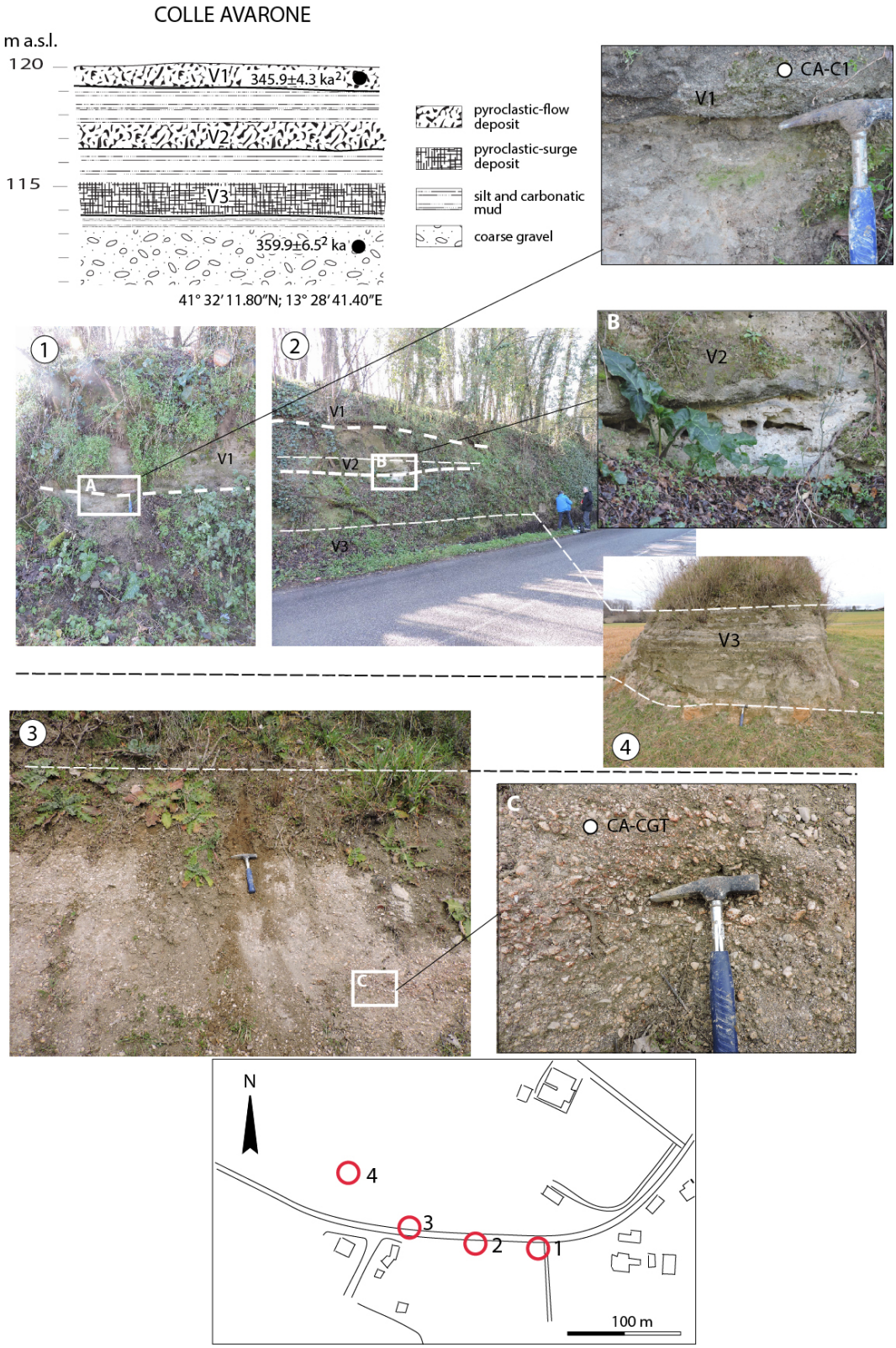

Figure S6 - Stratigraphic sketch of the composite Colle Avarone geological section. Photographs taken by author F. Marra. References: (2) Marra et al., 2021.

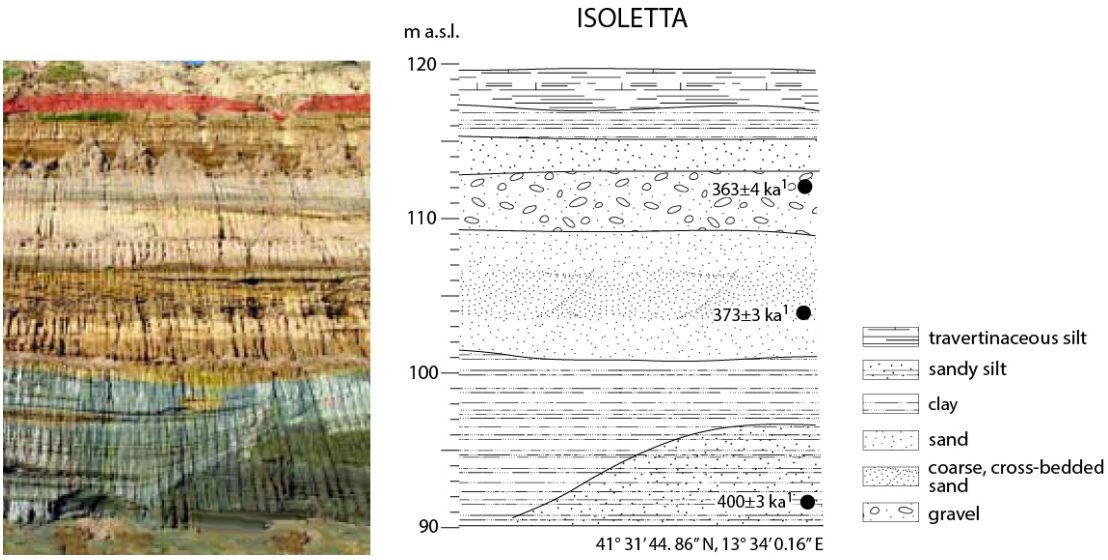

Figure S7 -Stratigraphic sketch of Isoletta geologic section. Photograph by author I. Biddittu. References: (1) Pereira et al., 2018.

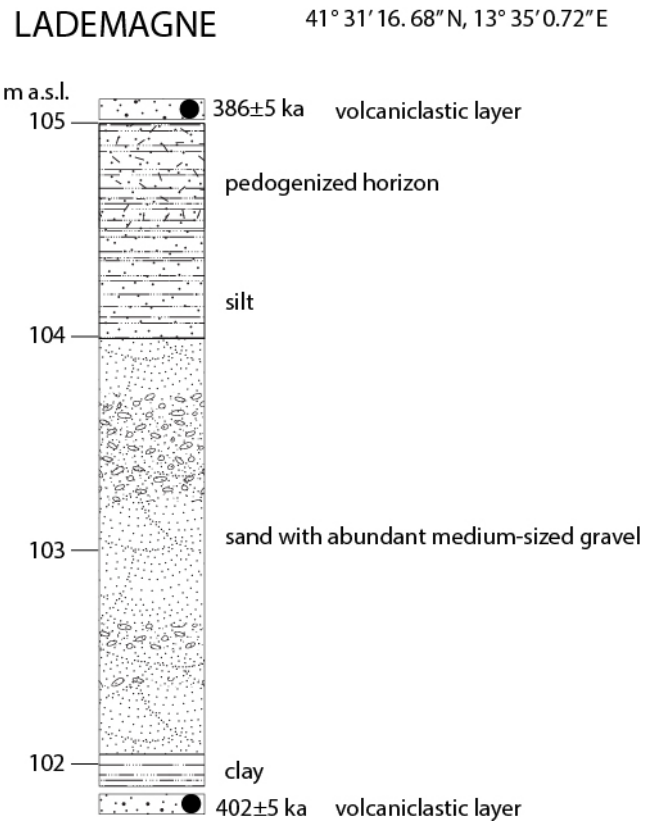

Figure S8 - Stratigraphic sketch of Lademagne geological section.

Figure S9 - Photograph taken by author I. Biddittu of the Pontecorvo outcrop showing occurrence of several tephra layers (arrow) intercalated in the Lower lacustrine succession. Two of these tephra layers were dated by K/Ar method (Narcisi, 1986).

REFERENCES

Marra, F., Cardello, L., Gaeta, M., Jicha, B., Montone, P., Niespolo, E., Nomade, S., Palladino, D.M., Pereira, A., De Luca, G., Florindo, F., Frepoli, A., Renne, P., Sottili, G., 2021. The Volsci Volcanic Field (central Italy): an open window on continental subduction processes, International Journal of Earth Sciences 110:689–718. DOI:10.1007/s00531-021-01981-6

Narcisi. B, 1986. Ricerche di tefracronologia nella media e bassa Valle Latina. Mem Soc Geol It 35, 909–912.

Pereira, A. *et al.* Geochronological evidences of a MIS 11 to MIS 10 age for several crucial Acheulian sites from the Frosinone province (Latium, Italy): Archaeological implications. *Quaternary Science Reviews* 187, 112-129 (2018).